

Attestation Waves: Platform Trust via Remote Power Analysis

Ignacio M. Delgado-Lozano¹, Macarena C. Martínez-Rodríguez²,
Alexandros Bakas¹, Billy Bob Brumley¹, and Antonis Michalas¹

¹ Tampere University, Tampere, Finland
{ignacio.delgado-lozano, alexandros.bakas}@tuni.fi
² Instituto de Microelectrónica de Sevilla,
CSIC/Universidad de Sevilla, Sevilla, Spain
macarena@imse-cnm.csic.es

Abstract. Attestation is a strong tool to verify the integrity of an untrusted system. However, in recent years, different attacks have appeared that are able to mislead the attestation process with treacherous practices as memory copy, proxy, and rootkit attacks, just to name a few. A successful attack leads to systems that are considered trusted by a verifier system, while the prover has bypassed the challenge. To mitigate these attacks against attestation methods and protocols, some proposals have considered the use of side-channel information that can be measured externally, as it is the case of electromagnetic (EM) emanation. Nonetheless, these methods require the physical proximity of an external setup to capture the EM radiation.

In this paper, we present the possibility of performing attestation by using the side-channel information captured by a sensor or peripheral that lives in the same System-on-Chip (SoC) than the processor system (PS) which executes the operation that we aim to attest, by only sharing the Power Distribution Network (PDN). In our case, an analog-to-digital converter (ADC) that captures the voltage fluctuations at its input terminal while a certain operation is taking place is suitable to characterize itself and to distinguish it from other binaries. The resultant power traces are enough to clearly identify a given operation without the requirement of physical proximity.

Keywords: attestation · remote power analysis · side channels · ADC · secure protocols · secure communications

1 Introduction

In our current network and interconnected world, establishing platform trust for execution of different security-critical operations is a need in diverse fields: examples include manufacturing, automation, communications, transport, work, and finance [5]. One approach is to use attestation mechanisms, which are suitable to verify the integrity of several elements such as application binaries, data,

or other internal platform state. Attestation normally consists of presenting a challenge by a verifier system that is already trusted to a prover system.

Attestation is a powerful concept to verify the integrity of untrusted systems. Recently, different attacks have appeared that aid in circumventing attestation by making a copy of the code that generates the checksum expected by the verifier (memory copy attack) [29, 30, 3], forwarding the challenge to another device that is able to compute the checksum properly (proxy attack) [15], or using return oriented programming gadgets to transiently hide the malicious code in parts of memory where the verifier cannot find it (rootkit attack) [2]. As a result, what we get are systems that are considered trusted by a verifier system, while the prover has bypassed the challenge.

To harden against these attacks on attestation methods and protocols, some proposals have considered the use of side-channel information that can be measured externally. For example, Sehatbakhsh et al. [28] recently utilized electromagnetic (EM) emanation to verify honest checksum computation. Nonetheless, these methods require proximity: a local external testbed set up near the prover in such a way that a carefully-placed probe can capture the EM radiation (traces) of the prover’s device. Furthermore, this testbed itself must be secured and trusted. The physical proximity requirement directly contradicts with the goals of remote attestation, not to mention failure to scale.

Recent trends in offensive cryptanalytic side-channel analysis are towards *remote power analysis* [19]. These techniques allow attackers to utilize pre-existing sensors or peripherals living in the same System-on-Chip (SoC) to procure traces. Regarding cryptanalytic side-channel attacks, this removes the physical proximity requirement from the threat model. In practice, these traces feature granularity reduced by several orders of magnitude when compared to traces captured with traditional high sampling rate oscilloscopes (e.g. 1MSPS in Section 3 vs. 40GSPS in [17]). Hence, remote power analysis trades this relaxed threat model for lower quality and higher quantity of traces. Section 2 contains more background on both remote power analysis and attestation.

In this paper, we propose utilizing remote power analysis for remote dynamic attestation, eliminating the physical proximity requirement of previous EM-based attestation proposals. Section 3 describes our testbed, with an application processor (AP) that executes the binary we aim to attest, by only sharing the Power Distribution Network (PDN) with the sensor that captures the traces. In our case, an analog-to-digital converter (ADC) captures the voltage fluctuations at its input terminal during attestation. Section 4 proposes an attestation protocol to establish secure communication between prover and verifier systems in a platform-agnostic way. Section 5 characterizes the degree to which the resulting traces captured from ADC vary over different binaries, with the goal of accurately matching traces to a priori applications with signal processing techniques via templating. In particular, we show that with a sufficient (yet small) number of traces, parameterized (in part) by various error rates, we are able to achieve excellent security levels and also understand the limitations of attestation in this novel setting. We conclude in Section 6.

2 Background

In a typical software-based attestation, a verifier is able to establish the absence of malware in a prover system with no physical access to its memory. This is possible because the verifier proposes a challenge to the prover, in which it must compute a checksum of its memory content. This challenge can only be correctly replied to if the memory content is not tampered, since the result of the checksum is only correct if the memory content within the prover system is exactly as expected by the verifier. For this, the verifier system needs to know several critical data about the prover, such as the clock speed, the instruction set architecture, the memory architecture of its microcontroller, and the size of its memories. This way, if in any moment a malicious prover aims to alter its memory, it is detectable by the verifier because the prover will present a wrong checksum result or a delay in the response [31]. This means that the integrity of the prover is verified, not only matching the checksum result with the expected result ($Response_{prover} = Response_{expected}$), but also through a parameter known as the request-to-response time ($t_{response} < t_{expected}$).

Numerous works focus on software-based attestation [29, 30, 3]. To threaten these attestation processes, several attacks have appeared during the last fifteen years that aim to break this attestation method. Attackers normally attempt to forge the response with a checksum computed in a different region of the prover memory that duplicates the code. This allows them to generate the expected response, which is known as a memory copy attack [29, 30, 3]. Another possibility is to forward the challenge to another device that is able to compute the checksum, then send it back to the verifier while satisfying the request-to-response time requirement, leading to proxy attacks. Li et al. [15] extensively describe proxy attacks and present attestation protocols to prevent them. The last option consists of storing the malicious code previous to the checksum calculation, by hiding it in other parts of the memory, allowing the prover to compute the correct checksum while the verifier is not able to detect the parts of the code that have been hidden, called a rootkit attack [2].

Along with software-based attestation processes, hardware-supported Trusted Execution Environments (TEE) are frequently used to ensure that the response of the computation is not tampered. Abera et al. [1] allow remote control-flow path attestation of an application without needing the code. They utilize ARM’s TrustZone (TZ) in order to avoid memory corruption attacks. de Clercq et al. [4] present a Control Flow Integrity (CFI) mechanism, guarding against code injection and code reuse attacks. They also present Software Integrity (SI) by storing precomputed MACs of instructions and comparing them with the MAC of the run-time execution. Moreover, Dessouky et al. [6] monitor every branch, a mitigation leveraging un-instrumented control-flow instructions.

Besides classical attestation, several recent works have used the EM emanations generated by a monitored system as a consequence of a certain execution within it, to detect malware in IoT devices. An example of this is EDDIE [21], a method that studies the spikes on the EM spectrum generated during a program execution and compares them to other peaks previously learned during a train-

ing stage. Significant differences in the spikes of EM spectrum allow to infer the introduction of malware in the studied program. Han et al. [13] give a similar approach, presenting ZEUS. This is a contactless embedded controller security monitor that is able to ensure the integrity of certain operations, by leveraging the EM emission produced during their execution, with no additional hardware support or software modifications. Yang et al. [32] and Liu and Vasserman [18] present very similar studies. The latter additionally considers the problem in terms of participants of an attestation protocol, namely, verifier and prover systems, although they do not develop a complete protocol itself. Msgna et al. [20] give another proposal that uses side-channel signals to check the integrity of program executions, where the use of power consumption templates is suitable to verify the integrity of code without previous knowledge about it. However, Sehatbakhsh et al. [28] propose the first attestation protocol based on EM signals with EMMA. The authors observe that execution time is only one of the multiple examples of using measurable side-channel information to gain knowledge about a specific computation, providing in many cases much finer-grain information than a unique temporal parameter. To develop this idea, they design a new attestation method based on the EM emanations generated by the prover while computing the checksum challenge proposed by the verifier, instead of the request-to-response time. After this, they show the implementation of this design, and consider and evaluate different attacks on EMMA. On the negative side, and opposed to classical attestation, this method requires physical proximity to the setup that captures the emanation, namely, a probe connected to an oscilloscope or external Software Defined Radio (SDR).

On a separate issue, several recent studies consider the possibility of attacking cryptosystems by using the side-channel information provided by mixed-signal components, such as ADCs [8, 22], or other sensors such as ring oscillators (ROs) [11, 33, 25] and time-to-digital converters (TDCs) [12, 9, 27, 26]. In real-world devices, these components are already placed in the same FPGA or SoC as a certain cryptographic module that is running some operations with secret parameters, or available through some interfaces present in processors, e.g. Intel Running Average Power Limit (RAPL) [16]. However, to the best of our knowledge, no study exists aiming to perform an attestation process by using the side-channel information captured by said components, leading to what we call *remote power analysis for attestation*. This technique features the benefits of the EM side channel (finer-grain information) without the negative sides (external setup with physical proximity).

3 Remote Power Analysis for Attestation

3.1 System description and measurements

As mentioned in the previous section, the goal of this work is to attest an operation run in a system by using the power leakage caused by the operation itself. In this context, where the power consumption traces can be acquired remotely, they can be used to attest an operation, because the procurement process can

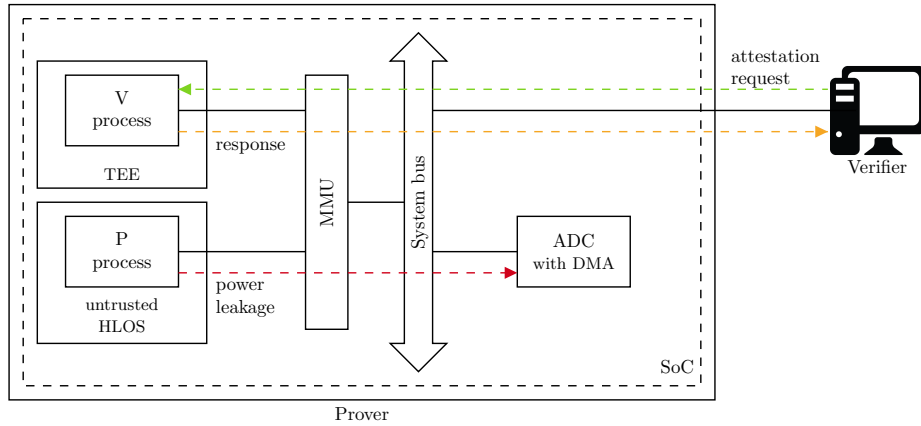


Fig. 1. Block diagram of the attestation process while running the operation.

be automated. Generally, the voltage fluctuations caused by the operation can be captured by any mixed-signal component, that could be an ADC, a sensor implemented on the programmable logic (PL), or any power supply monitor.

Figure 1 gives an overview of our system. It contains an AP where the operation (prover) and attestation (verifier) processes are run. Additionally, it contains the mixed-signal component that measures the supply voltage via ADC with Direct Memory Access (DMA) while the operation is run. The verification process saves the power trace captured by the mixed-signal component as binary data. Since we are using this side-channel trace data as evidence, the data must be trustworthy. Therefore, in our system, the ADC is inside the trust perimeter. Exactly how this happens in practice depends on the TEE technology. For example, on a platform that supports virtualization, this might be accomplished by a two-stage Memory Management Unit (MMU), where the hypervisor (or TEE) removes access from the untrusted High Level Operating System (HLOS) by simply not mapping the second-stage translation that would allow access to the ADC’s physical address space or the memory where it stores its data. This is indeed the scenario that Figure 1 depicts. On ARM-based SoCs this could also be accomplished with a Memory Protection Unit (MPU) that would be configured by a TZ-based TEE. The analogous upcoming technology for RISC-V would be Physical Memory Protection (PMP) [14]. So while the concrete protection mechanism on a given architecture depends on the TEE implementation, in this work we generically use the Linux kernel to simulate the TEE in terms of trust, and the kernel gates all userspace access to the ADC with traditional MMU-based access control.

Specifically, in this paper we conduct our experiments on a PYNQ-Z1 board. We programmed the FPGA of its Zynq 7000 chip to activate the ADC present on it, and capture the voltage fluctuations produced due to the execution of different operations inside the ARM Cortex-A9 processor. With this approach,

we aim to carry out the attestation process of an execution performed within the processor, simply with the side-channel information, given by the voltage fluctuations at the input of the ADC. This is present in the PL, and totally isolated from the AP core, having only a shared PDN as a common element.

The XADC module is a hard macro available in the FPGA of the Zynq 7000 chip. This module is not only an ADC converter of the analog data connected to the input channel, but it can also be configured to monitor the supply voltages and temperature. The XADC module supports multichannel, however we configure it with a single channel that monitors the internal core supply voltage. The output data size of this module is 16-bit data, with 12-bit precision. The sample rate is 1MSPS. The 32-bit AXI streaming output of the XADC is used to transfer as many samples as possible to the AP. The XADC outputs samples on the AXI Stream for each of its channels when it is enabled, in this case, only one channel. We use DMA transfer from the PL to the AP to move XADC samples into the AP memory, and we use an AXI GPIO to set the size of the transfer. Since the width of the AXI stream is double the output data size, there are two measurements at each memory position.

During the attestation process, first the number of power measurements to be captured is set: that is, the buffer size. Just before running the operation, the DMA is enabled, then we run a trigger operation to indicate in the signal the beginning of the operation to be attested, then the operation itself is run, and finally, another trigger operation indicates that it has ended. The XADC is capturing power data until the DMA transfer is completed. The AP reads the part of the memory where the measurements are stored and processes it as needed.

We summarize our procurement process as follows, that saves the power traces as binary data used in the attestation protocol. (i) Set the buffer size; (ii) enable the DMA engine; (iii) send the start trigger; (iv) execute the target binary; (v) send the end trigger; (vi) wait for the DMA to complete; (vii) process the resulting binary data (trace). In practice, the (untrusted) HLOS executes step (iv) and the TEE executes all other steps.

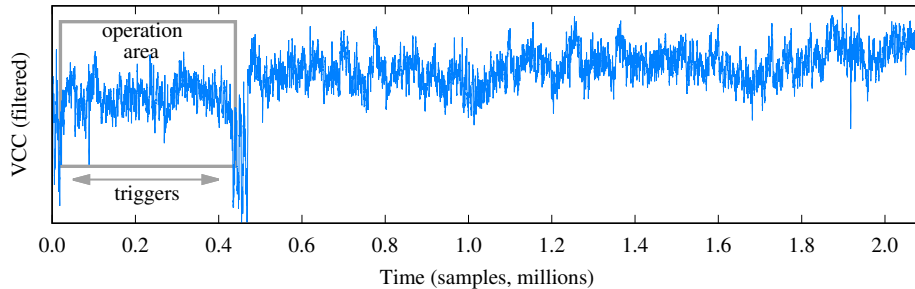


Fig. 2. Example of a power trace captured with the XADC.

Figure 2 shows a power trace captured with the XADC while an operation is run. The two trigger operations are shown at the beginning and the end of the operation, determining the operation area. The rest of the trace is the value of the supply voltage after the operation is finished. This trace is subsequently processed in the protocol to attest the operation.

4 System Model and Protocol Construction

In this section, we demonstrate how our attestation technique can be applied and used in real-life deployments and not remain just a lab-concept. To this end, we present a detailed protocol showing the communication and all the messages exchanged between the involved entities. Our protocol description includes the definition of the underlying system model, as well as the presentation of all the involved entities and their specifications. Finally, we construct our threat model and show our protocol’s resistance against a powerful malicious adversary \mathcal{ADV} . While this is not the core contribution of this work, we consider it an important part since it tackles a problem so far only dealt with at a high level in other similar works (e.g. [28]). We believe our approach can provide an impetus towards paving the way for the integration of our, or similar, techniques in existing services.

4.1 System Model

We assume the existence of the following components:

Verifier (\mathcal{V}): Here, verifier is a user who wishes to execute a piece of software on an untrusted platform. Prior to exchanging the data with the untrusted platform, the user needs to verify its trustworthiness.

Prover (\mathcal{P}): The prover is an untrusted platform that needs to convince a verifier of its trustworthiness. It consists of an untrusted application and a TEE.

1. **Untrusted application:** The application handles the communication between the verifier and the untrusted platform. After proving its trustworthiness, the application will be responsible for executing software specified by the user.
2. **Trusted Execution Environment:** We assume the existence of a TEE residing either on the untrusted platform or in a remote location. The TEE is invoked by the untrusted application upon receiving an attestation request by a verifier. TEE’s main responsibility is to measure the power consumption of the untrusted part of \mathcal{P} , while running an application requested by \mathcal{V} . (Here we recall that the TEE also hosts the component that takes the measurements.)

Measurements Tray (MT): MT is an entity residing in the cloud. Its main responsibility is to store templates and compare them with traces that are received by \mathcal{V} . There are two separate reasons that led us to have MT as an independent component and not as a part of \mathcal{V} . (i) MT residing on \mathcal{V} 's side would result in higher local storage costs, as \mathcal{V} would have to keep a copy of each template locally. (ii) Assuming that MT is an independent cloud component, all MT updates are executed centrally. This eliminates the need for separate updates.

4.2 Attestation Protocol

Having defined our system model, we can now proceed to describe our attestation protocol. Our construction is divided into three phases: the *Setup Phase*, the *Trusted Launch Phase* (Figure 3), and the *Computations Phase* (Figure 4). For the rest of this paper, we assume the existence [10] of an IND-CCA2 secure public key cryptosystem, EUF-CMA secure signature scheme, and a first and second preimage resistant hash function $H(\cdot)$.

Setup Phase: During this phase, each entity receives a public/private key pair. More specifically:

- $(\text{pk}_{\mathcal{V}}, \text{sk}_{\mathcal{V}})$ - Verifier \mathcal{V} 's public/private key pair.
- $(\text{pk}_{\mathcal{P}}, \text{sk}_{\mathcal{P}})$ - Prover \mathcal{P} 's public/private key pair.
- $(\text{pk}_{\text{MT}}, \text{sk}_{\text{MT}})$ - MT's public/private key pair.

Trusted Launch Phase: In this phase, \mathcal{V} wishes to launch a TEE on the untrusted platform. The TEE will be responsible for measuring the power consumption while \mathcal{P} executes applications of \mathcal{V} 's choice. To facilitate \mathcal{V} , we assume the existence of a setup function F_s , responsible for setting up the TEE³. Finally, we further assume that the setup function F_s is publicly known.

This phase commences with the verifier \mathcal{V} generating a random number r_1 and sending $m_1 = \langle r_1, A \rangle$ to \mathcal{P} , where A is the unique identifier of the application that \mathcal{V} wishes to execute on the TEE. Moreover, \mathcal{V} captures the current time t_1 . Upon reception, \mathcal{P} calculates $\text{checksum}(r_1, F_s)$, and gets the result res . After the successful execution of F_s , a new TEE is launched on the untrusted platform. Upon its creation, the TEE also obtains a public/private key pair $(\text{pk}_{\text{TEE}}, \text{sk}_{\text{TEE}})$ (sealing/unsealing keys). The result of the checksum will be then sent back to \mathcal{V} along with the launched TEE's public key. More precisely, \mathcal{P} sends the following message to \mathcal{V} : $m_2 = \langle r_2, \text{Enc}_{\text{pk}_{\mathcal{V}}}(\mathcal{P}, \text{res}, \text{pk}_{\text{TEE}}), \sigma_{\mathcal{P}}(H_1) \rangle$, where $H_1 = H(r_2 || \mathcal{P} || \text{res} || \text{pk}_{\text{TEE}})$. Upon reception, \mathcal{V} captures the time t_2 and calculates $\Delta t = t_2 - t_1$ (possible because \mathcal{V} also knows the function F_s). If Δt is as expected, then \mathcal{V} knows that there is a TEE residing on the untrusted platform. Figure 3 illustrates this phase.

³ The specifications of F_s will be TEE-dependent. However, it must be designed in such a way that any manipulation will create a noticeable time increase in the computation of the checksum.

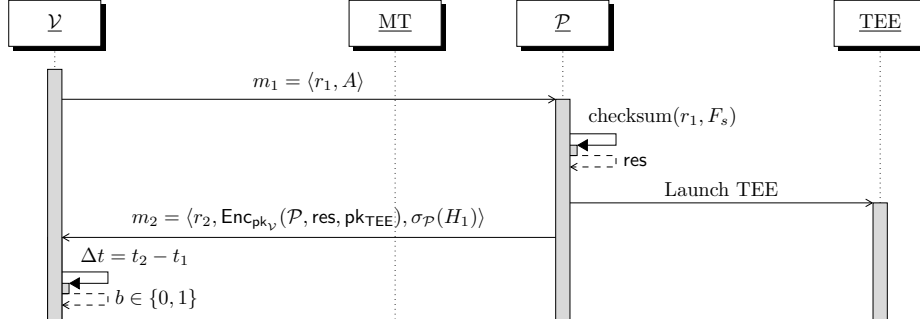


Fig. 3. Trusted Launch Phase.

Computations Phase: After the successful execution of the Trusted Launch Phase, \mathcal{V} is convinced that a newly launched TEE is residing on the untrusted platform. \mathcal{V} wishes to run an executable application A on the untrusted part of \mathcal{P} . To ensure that the results will be accurate, \mathcal{V} first decides the number of required traces. This decision depends on the statistical results described later (Section 5). After deciding the number of runs n , \mathcal{V} initiates the protocol. To this end, \mathcal{V} first generates a token τ and a fresh random number r_3 , and contacts \mathcal{P} by sending $m_3 = \langle r_3, n, \tau, A, \sigma_{\mathcal{V}}(H_2) \rangle$, where $H_2 = H(r_3 || \tau || A || n)$ and A is the unique identifier of the application that \mathcal{V} wishes to execute on \mathcal{P} . Upon reception, \mathcal{P} starts running application A n times with τ as input, and produces an output out , and a fingerprint $H(\tau, A)$. Simultaneously, the TEE measures the power consumption of the untrusted part of \mathcal{P} to get a sequence of traces $\{tr_i\}_{i=1}^n$ (one for each execution of A). As soon as \mathcal{P} outputs out , it sends an acknowledgement ack to the TEE. Upon reception, the TEE will reply to \mathcal{P} with $m_4 = \langle r_4, \text{Enc}_{\text{pk}_{\mathcal{V}}}(\{tr_i\}_{i=1}^n), \sigma_{\text{TEE}}(H_3) \rangle$, where $H_3 = H(r_4 || tr_1 || \dots || tr_n)$. \mathcal{P} will finally send $m_5 = \langle r_5, m_4, H(\tau, A), \text{out}, \sigma_{\mathcal{P}}(H_4) \rangle$, where $H_4 = H(r_5 || m_4 || \text{out})$. Upon receiving m_5 , \mathcal{V} verifies the signatures of the TEE and \mathcal{P} , and the freshness of both m_4 and m_5 messages. After the first successful execution of the protocol, \mathcal{V} commences a fresh run, until she gathers all the required traces. When \mathcal{V} gets the desired number of traces, she generates $m_6 = \langle r_6, \text{Enc}_{\text{pk}_{\text{MT}}}(\tau, \text{out}, A, \{tr_i\}_{i=1}^n), \sigma_{\mathcal{V}}(H_3) \rangle$, where $H_3 = H(r_6 || \tau || A || \text{out} || \{tr_i\}_{i=1}^n)$ and sends it to MT. MT can then check the trust level of \mathcal{P} by comparing out and each tr_i against its pre-computed list of measurements. Finally, MT outputs a bit $b \in \{0, 1\}$ and sends $m_7 = \langle r_7, \text{Enc}_{\text{pk}_{\mathcal{V}}}(b), \sigma_{\text{MT}}(H_4) \rangle$, where $H_4 = H(r_7 || b)$ to \mathcal{V} . Figure 4 depicts the Computations Phase.

4.3 Threat Model

Our threat model is based on the Dolev-Yao adversarial model [7]. Furthermore, we assume that \mathcal{ADV} can load programs of her choice in the enclaves and observe their output. This assumption significantly strengthens \mathcal{ADV} since we need to

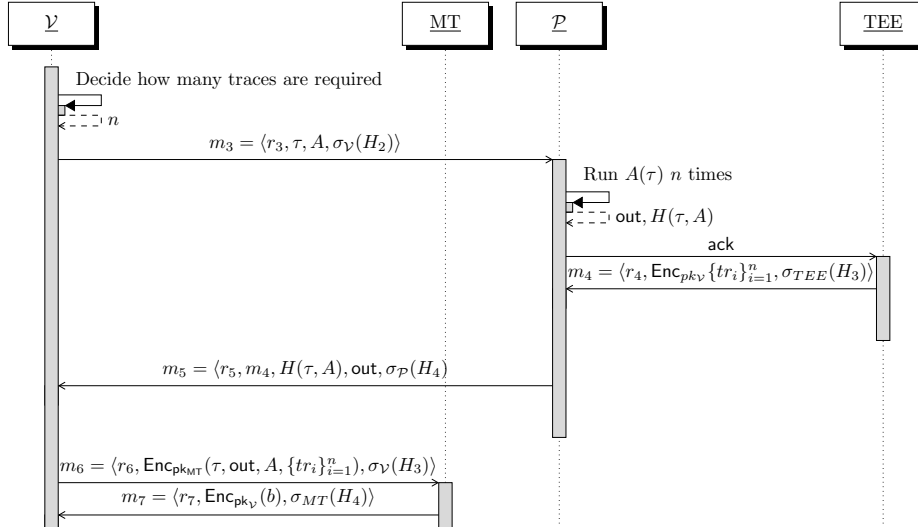


Fig. 4. Computations Phase: we assume \mathcal{P} and the TEE reside on the same platform.

ensure that such an attack will not be detectable from \mathcal{V} 's point of view. Finally, we extend the above threat model by defining a set of attacks available to \mathcal{ADV} .

Attack 1 (Measurements Substitution Attack) *Let \mathcal{ADV} be an adversary that has full control of the untrusted part of \mathcal{P} . \mathcal{ADV} successfully launches a Measurements Substitution Attack if she manages to substitute the measurements received from TEE by some others of her choice, in a way that is indistinguishable for \mathcal{V} .*

Attack 2 (False Result Attack) *Let \mathcal{ADV} be an adversary that overhears the communication between \mathcal{V} and MT. \mathcal{ADV} successfully launches a False Result Attack if she can tamper with the response sent from MT to \mathcal{V} .*

While the first two attacks target directly the protocol communication, we also define a third attack that aims at targeting a false positive (FP) case, analyzed further in Section 5. An adversary could exploit the FP by substituting \mathcal{V} 's application with another of her choice. The resulting trace, even if it comes from a different application, could still pass as valid by \mathcal{V} .

Attack 3 (Application Substitution Attack) *Let \mathcal{ADV} be an adversary that overhears the communication between \mathcal{V} and \mathcal{P} . \mathcal{ADV} successfully launches an Application Substitution Attack if she manages to replace the trace that \mathcal{V} is expecting with another of her choice, with non-negligible advantage, where the advantage of \mathcal{ADV} is defined to be the following conditional probability:*

$$\text{Adv}_{\mathcal{ADV}} = \Pr[\mathcal{V} \text{ accepts the trace} \mid \mathcal{ADV} \text{ switched the application}]$$

4.4 Security Analysis

We now prove the security of our protocol in the presence of a malicious adversary \mathcal{ADV} as defined in Section 4.3.

Proposition 1 (Measurements Substitution Attack Soundness). *Let \mathcal{ADV} be an adversary that has full control of the untrusted part of \mathcal{P} . Then \mathcal{ADV} cannot perform a Measurements Substitution Attack.*

Proof. For \mathcal{ADV} to successfully launch a Measurements Substitution Attack, she needs to replace the measurements μ , with some other measurements μ' of her choice. To do so, \mathcal{ADV} can either generate a fresh μ' , or replay an old one. In both cases, \mathcal{ADV} must generate a message $m_5 = \langle r, m_4, H(\tau, A), \text{out}, \sigma_{\mathcal{P}}(H(r||m_4||\text{out})) \rangle$. It is clear from the message structure, that the only component that \mathcal{P} cannot forge, is the message m_4 included in m_5 . As m_4 is signed by the TEE, and given the EUF-CMA security of the signature scheme, \mathcal{ADV} can only forge the TEE's signature with negligible probability. Hence, the only alternative for \mathcal{ADV} is to use an older m_4 message that she received from the TEE sometime in the past. Let $m_{4_{old}}$ be the old m_4 message such that $m_{4_{old}} = \langle r_{4_{old}}, \text{Enc}_{pk_{\mathcal{V}}}(\mu), \sigma_{TEE}(H_3) \rangle$, where $H_3 = H(r_{4_{old}}||\mu')$. While this approach solves the problem of forging TEE's signature, \mathcal{ADV} now needs to further tamper with this message by replacing $r_{4_{old}}$, with a fresh random number. This is important because otherwise, \mathcal{V} will not be able to verify the freshness of the message, and will thus abort the protocol. However, $r_{4_{old}}$ is included in the signed hash of the TEE, and given the second preimage resistance of the hash function H we have that $H(r, \mu') \neq H(r', \mu') \forall r, r'$ such that $r \neq r'$. Hence, \mathcal{V} realizes that something is wrong and aborts the protocol.

Proposition 2 (False Result Attack Soundness). *Let \mathcal{ADV} be a malicious adversary that overhears the communication between \mathcal{V} and MT. Then \mathcal{ADV} cannot successfully perform a False Result Attack.*

Proof. For \mathcal{ADV} to launch a False Result Attack, she needs to forge the message m_6 sent by MT to \mathcal{V} in a way that \mathcal{V} will not be able to distinguish any difference. To do so, \mathcal{ADV} has two choices: (i) substitute the encrypted bit, with a bit of her choice; (ii) replay an older message.

Substituting the encrypted result is feasible since \mathcal{V} 's public key is publicly known. Hence, it is straightforward for \mathcal{ADV} to encrypt a bit under $pk_{\mathcal{V}}$ and replace it with the actual encrypted result. However, since the encrypted bit is also included in the signed hash, \mathcal{V} will be able to ascertain that the integrity of the message has been violated. Thereupon, for \mathcal{ADV} to successfully substitute the encrypted bit, she needs to also forge the MT's signature. Given the EUF-CMA security of the signature scheme, this can only happen with negligible probability and so, the attack fails.

Insomuch as \mathcal{ADV} overhears the communication between \mathcal{V} and MT, she has knowledge of the random numbers used to ensure the freshness of the messages. On that account, \mathcal{ADV} could try to forward to \mathcal{V} an older m_7 message, with

a fresh random number. However, just like in the previous case, the random number is also included in the signed hash, and consequently \mathcal{ADV} would once again have to forge the MT's signature, which can only happen with negligible probability.

The above proofs support our claim that in both cases the attack can only succeed with negligible probability. As a result, \mathcal{ADV} cannot successfully launch a False Result Attack.

Proposition 3. *Let n be the total number of traces captured to perform an attestation process. Let p_α be the probability of an attacker obtaining a success result with a single trace derived from another operation, and p_β the honest user success probability, using a single trace coming from the appropriate operation. Assuming that $p_\beta > p_\alpha$, there exists a threshold number of traces, x_{th} , required to pass the attestation process, for which $P(\alpha) = 0$ and $P(\beta) = 1$, using a sufficiently large number n of traces.*

Proof. Let $\{X_i\}$ be a succession of independent random variables that take one of two different results:

$$X_i = \begin{cases} 0, & \text{do not pass the attestation process} \\ 1, & \text{pass the attestation process} \end{cases}$$

Let $x = \sum_{i=1}^n X_i$ be the number of times we pass the attestation process. We know, by the strong law of large numbers (SLLN) that:

$$P\left(\lim_{n \rightarrow \infty} \frac{\sum_{i=1}^n X_i}{n} = E(X_i)\right) = 1 \quad (1)$$

where $E(X_i)$ is the expected value of variable X_i . From the binomial distribution formula:

$$P(x) = \binom{n}{x} \cdot p^x \cdot (1-p)^{n-x} \quad (2)$$

Leveraging that, in the binomial distribution, the expected value $E(X_i)$ of a variable matches with its probability p . We can substitute in Equation 1, yielding:

$$P\left(\lim_{n \rightarrow \infty} \frac{\sum_{i=1}^n X_i}{n} = p\right) = 1 \Rightarrow P\left(\lim_{n \rightarrow \infty} \frac{x}{n} = p\right) = 1$$

Let us consider now the two different cases of p_α and p_β . For a sufficiently large n , we get that:

$$P\left(\lim_{n \rightarrow \infty} \frac{x_\alpha}{n} = p_\alpha\right) = 1 \Rightarrow \lim_{n \rightarrow \infty} \frac{x_\alpha}{n} = p_\alpha \text{ almost surely}^4 \quad (3)$$

$$P\left(\lim_{n \rightarrow \infty} \frac{x_\beta}{n} = p_\beta\right) = 1 \Rightarrow \lim_{n \rightarrow \infty} \frac{x_\beta}{n} = p_\beta \text{ almost surely} \quad (4)$$

⁴ Notice that ‘‘almost surely’’ is a concept used in probability theory to describe events that occur with probability 1 when the sample space is an infinite set.

Since $p_\beta > p_\alpha$ by assumption (an essential condition to perform a solid attestation), we can select x_{th} defined as the threshold number of traces such that $p_\alpha < \frac{x_{th}}{n} < p_\beta$ for which we need a number $\frac{x}{n} \geq \frac{x_{th}}{n}$ to have a positive result of the attestation process. Then, from Equation 3 and the fact that $p_\alpha < \frac{x_{th}}{n}$ by definition, we get:

$$P(\alpha) = P\left(\lim_{n \rightarrow \infty} \frac{x_\alpha}{n} \geq \frac{x_{th}}{n}\right) = 0$$

Analogously, from Equation 4 and the fact that $p_\beta > \frac{x_{th}}{n}$ by definition, we get:

$$P(\beta) = P\left(\lim_{n \rightarrow \infty} \frac{x_\beta}{n} \geq \frac{x_{th}}{n}\right) = 1$$

5 Evaluation

With the previous sections explaining how we capture the traces from the ADC and how we establish security between the prover and the verifier system, we are in a position to explain our experiments. We open with a description of our analysis framework, including empirical evaluation (Section 5.1). We then close with a security analysis of the different framework parameters (Section 5.2), guiding selection when instantiating the Section 4 protocols.

5.1 Methodology

Our procedure consists of (i) selecting the traces generated by the ADC that belong to a given program; (ii) generating a template by averaging a large number of traces; and (iii) comparing this template to different traces, some that belong and some that do not to the same given program. Our methodology uses profiling both to build the templates and calculate the correlation threshold that operations should surpass to complete the attestation, both which vary across binaries (see Table 2). As an alternative, non-profiled approaches could be an interesting research direction to potentially improve scalability and agility. We utilize the Pearson correlation for our comparison metric. These, ultimately, will lead to statistics about the true positive (TP), true negative (TN), false negative (FN), and false positive (FP) rates that will allow us to make a concrete analysis concerning the suitability of the traces retrieved by a given sensor or peripheral to perform attestation. From this data, we obtain the following parameters, which are typical in information classification, that give an idea of the accuracy and relevance of our experiments.

$$Precision = \frac{TP}{TP + FP} \quad Recall = \frac{TP}{TP + FN} \quad F1 = 2 \cdot \frac{Recall \cdot Precision}{Recall + Precision}$$

This way, precision gives a measure of the number of correct results among all the returned results, while recall gives a measure of the number of correct results divided by the number of results that should have been returned. This means that a low result of precision implies that a high number of incorrect results are considered as correct, so our system would be yielding many FP. On the other

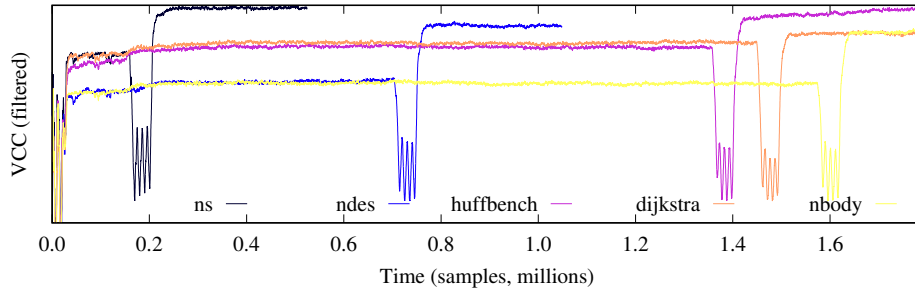


Fig. 5. Several templates selected, with different number of samples.

hand, a low recall implies that we are not considering as correct some results that indeed are correct, leading then, to a high number of FN. Finally, F1 is the harmonic mean between recall and precision, and allows us to give an idea of how good our system is at retrieving results with one single measurement.

Specifically, we utilize the executables in the Bristol Energy Efficiency Benchmark Suite (BEEBS) [23, 24], providing a broad spectrum of programs⁵ to profile w.r.t. our methodology. We execute the BEEBS programs and capture their traces from the ADC in order to perform attestation by comparing each trace with templates previously obtained for the other BEEBS programs. The aim is that a trace coming from a certain program only matches (leading to a high correlation value) with the template belonging to its own program and does not match (yielding a low correlation value) with other programs' templates.

To accomplish this, we first capture 1000 traces from each program and generate templates from them. Then, we apply a Savitzky-Golay filter to obtain the final template. Figure 5 depicts the final template of five BEEBS programs, where the trigger operations determine each program operation area (see Figure 2). It is important to notice that the amplitude shift in the traces is not a reliable differentiator, since it depends on the moment the traces are taken.

One observation from Figure 5 is that the templates associated to each program take different times, translated into different number of samples, to complete their execution. The program will be running while the ADC is capturing samples between the start and the ending trigger. The rest of the trace after the end trigger is simply noise. Our ADC captures 2^{21} samples for every trace and template, but in order to perform the correlations, each program and its template are separated into different groups according to their lengths ranging from 2^{17} to 2^{21} samples. This way, depending on the length of the different templates, we keep the execution part from the traces and templates by selecting a number of samples between 2^{17} to 2^{21} samples, trying to catch the relevant information from said execution. Since the rest of the trace, once the program is executed and finished, is simply noise, we discard it.

⁵ <https://github.com/mageec/beebs>

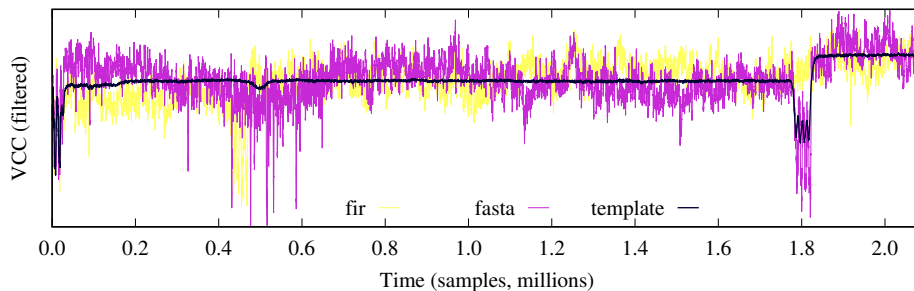


Fig. 6. Matching of the fasta template (black) with two different traces (fasta, fir).

After computing all the templates, our experiment consists of capturing 1000 traces for every program and comparing them against their own template. To achieve this, we compute the Pearson correlation between every trace of the program selected and its template. We store this in a correlation vector $corr_{vector} = (corr_1, corr_2, \dots, corr_{1000})$, then the components of $corr_{vector}$ are ordered from smallest to largest, in order to compute the 25th percentile. This is to say, we compute a threshold value $corr_{thres}$ from which 750 components of the vector are above it. In practical terms, this means that during the matching stage, a trace that has a correlation value above the threshold will be considered as representative of an honest execution from a certain program, while a trace with a correlation value lower than this threshold cannot certify that the trace belongs to the program related to the template. This matching stage, in practical terms, works as a training set for our correlation system where we select a threshold value that let pass the 75% of the traces from that matching set. When we move to the evaluation stage, the threshold value is the one that we previously selected, but it does not need to pass exactly the 75% of the traces, since the traces from the evaluation stage are not the same as the one from the matching stage. Nonetheless, it should yield a similar ratio of traces that pass the attestation. This way, we ensure that the threshold admits a sufficient number of traces, without allowing a large number coming from other operations. In Figure 6, it is visible to the naked-eye how a correct trace matches with its template, against a trace that does not belong to the program according to the used template.

After this, we select a template and compute correlations for all the BEEBS executables, with a set of 1000 traces from each program. If traces that do not belong to the program being checked match with the corresponding template, having a correlation value higher than the threshold, we will have a FP. On the contrary, if a trace that belongs to this program does not match with its own template, having a correlation value lower than the threshold, we will have a FN. From these statistics, we compute recall, precision, and F1 score as previously defined. To obtain those statistics, we first trim the traces to have the same number of samples than the template used in each case, in order to be able to compute the Pearson correlation value between the traces and the given tem-

plate. Figure 7 illustrates the whole process, repeated for the templates obtained from each program. We verified that this process can be carried out even if the templates are generated from a set of data from a given board of a certain model, and the evaluation stage where we compute the correlation of the traces with the templates previously generated are captured from a different board of the same model. This characteristic demonstrates the robustness of our attestation protocol, and its utility in systems where we can have pre-loaded templates for given binaries coming from different devices.

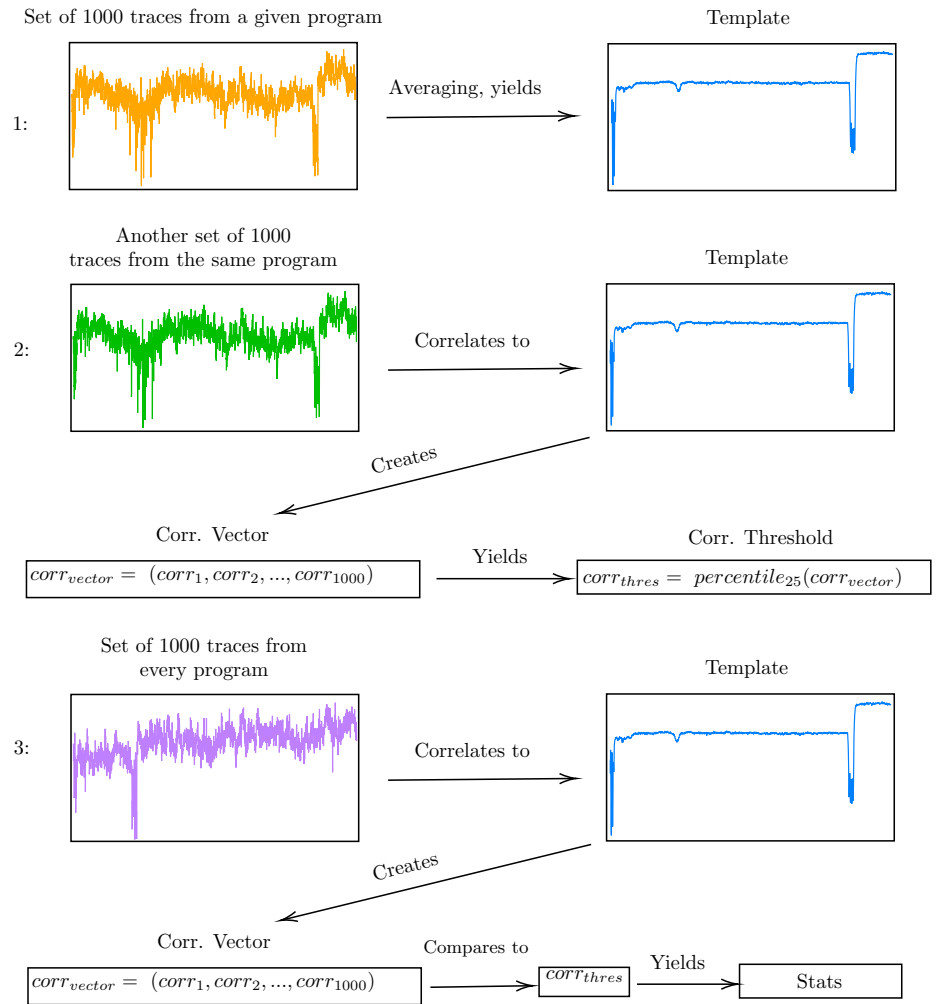


Fig. 7. Process repeated with every template to obtain statistics.

We present the complete statistics in Table 2. It includes the correlation threshold value for each program, the name of the program that yields the highest FP rate, the absolute number out of the 1000 traces that provides a correlation value higher than the threshold (leading to FP), recall, precision, and F1 score metrics. From Table 2, we can see that out of 47 programs, 35 have a precision above 0.90 and 42 above 0.80, while 27 programs have a recall above 0.70 and 44 above 0.60. Thus, our method correctly distinguishes positive results among the total number of traces, having in general a low FPR, and leading to excellent precision values. On the contrary, the recall results are lackluster, meaning that a significant portion of correct results are not retrieved by our system, leading to an improvable FN rate (FNR).

Another concern is the fact that out of 1000 traces, in the worst FP case scenario from a specific benchmark, 82 traces from `ndes` program are considered as correct results by the `nettle-aes` template, leading to a FPR of 8.2 % from that specific operation. This means that traces coming from a given operation are likely useful to attest others. The consequences, at this point, are clear. To have said 8.2 % of FP results, would lead to an inadmissible number of incorrect traces passing the attestation process. This is especially worrying, taking into account that the recall (which is equivalent to TPR, the TP rate) is 69 %. With these results, each time we want to use this attestation process, we have roughly a 3/10 probability of failing even if the computations are carried out properly, and around a 1/12 probability of having a correct result in cases where the retrieved trace matches with the template, even if it does not belong to the correct program. This is far from the aimed numbers to perform solid attestation using our proposal.

5.2 Parameterization

To overcome these deficiencies, we can use several traces to perform the attestation. We aim to improve these numbers by requiring that out of n traces, a minimum number x_{th} must be above the threshold correlation value. Proposition 3 presents the general case, but now we must assign discrete values to the various parameters.

For our case, and to obtain a good trade-off between the probabilities of having FPs that pass the attestation, and having FNs that are not able to pass even if they belong to the correct template, we consider the following threshold. It is the midpoint of p_α and p_β , recalling those parameters from Proposition 3.

$$x_{th}, n \in \mathbb{N} : x_{th} = \left\lceil n \cdot \frac{p_\alpha + p_\beta}{2} \right\rceil \wedge p_\alpha < \frac{x_{th}}{n} < p_\beta$$

It is important to notice that each user can freely select this threshold number of traces by, for example, giving different weights to p_α and p_β or selecting a totally different relation. As previously indicated, we select this threshold to have a good trade-off between an attacker trying to cheat the attestation process with a trace coming from another operation and an honest user.

Moreover, the user determines the security level by selecting an appropriate number of total traces n . Here, we understand the security level as a measure of the probability of passing the attestation protocol using traces coming from a different operation, given the number of traces required to be above the correlation threshold and the total number of traces n . Larger values of n tend to minimize the FP probabilities and increase the corresponding TP probabilities (thus, reducing also FNs). For our worst FP scenario coming from a specific benchmark, we have 82 traces out of 1000 coming from the ndes benchmark that yield FP results using the nettle-aes template. On the other hand, the TPR for nettle-aes is 0.69. In this case, we can identify the FPR from the ndes traces, with an attacker’s probability to successfully cheat the attestation process of the nettle-aes operation, thus, $p_\alpha = 0.082$. Analogously, the TPR for nettle-aes is the success probability of an honest user, thus $p_\beta = 0.69$. Iterating, we found that for $n = 243$ traces, the threshold needed to pass the attestation is:

$$x_{th} = \left\lceil 243 \cdot \frac{0.69 + 0.082}{2} \right\rceil = 94$$

Combining our results for the obtained threshold with the binomial distribution (Equation 2) for $n = 243$ and $p_\alpha = 0.082$, we get that the probability to cheat the attestation is:

$$P(\alpha) = P(x \geq 94) = P(94) + P(95) + \dots + P(243) \text{ using } p_\alpha = 0.082$$

$$P(\alpha) = 3.72 \cdot 10^{-39} \approx \frac{1}{2^{128}} = 2.94 \cdot 10^{-39}$$

which is equivalent to a 128-bit security level. Using only 243 traces to complete the attestation process is a very promising result, especially since this is only a proof-of-concept of our novel attestation approach.

Considering the TPR, for $n = 243$ traces and $p_\beta = 0.69$, we get that:

$$P(\beta) = P(x \geq 94) = P(94) + P(95) + \dots + P(243) \text{ using } p_\beta = 0.69$$

$$P(\beta) = 1 - 6.27 \cdot 10^{-23} \approx 1 - \frac{1}{2^{74}}$$

Thus, we achieve an (almost) perfect TPR with the selected number of traces. It is important to notice that these 243 traces are needed in our worst case scenario. Concretely, our worst case scenario is that in which a higher number of traces coming from a different operation passes the attestation process of another binary. For the rest of binaries, the security level achieved will be equal or better than this one. Table 1 show similar results about the number n of traces and the threshold x_{th} required to pass the attestation with various security levels for this worst case scenario.

Ideally, we would achieve a certain security level by isolating the minimum number n of traces and the x_{th} required to find a given $P(\alpha)$. However, this is not possible, since the inverse function of the binomial cumulative distribution does not exist. In other words, there is not an analytical form to find n starting

Table 1. Parameter variations to achieve different security levels.

Security Level	n	x_{th}	$P(\alpha)$	$P(\beta)$
32-bit	52	21	$2.39 \cdot 10^{-10} \approx 2^{-32}$	$1 - 5.43 \cdot 10^{-6} \approx 1 - 2^{-17}$
64-bit	114	45	$5.18 \cdot 10^{-20} \approx 2^{-64}$	$1 - 2.22 \cdot 10^{-11} \approx 1 - 2^{-35}$
128-bit	243	94	$3.72 \cdot 10^{-39} \approx 2^{-128}$	$1 - 6.27 \cdot 10^{-23} \approx 1 - 2^{-74}$
256-bit	494	191	$9.83 \cdot 10^{-78} \approx 2^{-256}$	$1 - 4.14 \cdot 10^{-44} \approx 1 - 2^{-144}$

from a given $P(x_{th} \geq x)$. That is the reason why we use the iteration approach, through readily-available numerical methods that are easily and fastly computed by any tool or programming language considering the equation from the binomial distribution.

6 Conclusion

The main contribution of this paper is the proposal of a new method to verify the integrity of a SoC, by natively capturing the side-channel leakage produced during the execution of a given operation. In our case, an ADC present in an FPGA adjacent to the AP carrying out the operation that aims to be verified is suitable to measure the voltage fluctuations caused by the execution itself. These voltage fluctuations are able to characterize the performed operation and to distinguish it from other binaries.

This attestation method does not rely on the request-to-response time, using instead the power signal generated by the program execution, which provides more detailed information about what its proper behavior should be. Additionally, our method does not require an external setup with physical proximity to capture the side-channel vector, rather native components. Thus, it implies no software or hardware overhead to the system, since it simply internally captures a power trace while carrying out executions in a normal operating mode.

To end, our attestation protocol completes the work. It describes not only how our system can capture the power leakage that allows us to characterize a given operation, but also how to manage the resultant power trace to, realistically, verify the integrity of an untrusted system. This achieves our main goal: checking that an untrusted system is executing programs honestly, without the presence of any malware. As far as we are aware, our work is the first constructive application of remote power analysis, identified as an open problem in [19].

Limitations and future work. Our proof-of-concept work exhibits a variety of limitations that should be addressed in future related studies. A brief summary follows. (i) TP rates are improvable, especially taking into account that our traces are fairly noisy. Nonetheless, using several power traces we are able to overwhelmingly detect honest users vs. attackers. (ii) Substitution attacks are a real threat, in case the ADC resolution is not sufficient to capture malicious modifications in the instructions from a binary. Future work includes exploring

attacker strategies to modify binaries to produce power traces that pass attestation. (iii) The matching between traces and templates are mainly based in the duration of the executed operation, since we use the ending triggers as a distinctive mark in the power traces. However, the fact of using a whole power trace (vectorial data) instead of the classical request-to-response time (scalar data) hardens proxy attacks, because an attacker does not only need to solve a challenge in a given time, but to generate a power trace similar to the template, which is a difficult challenge. (iv) Consulting Figure 1, a natural observation is that requiring a TEE for dynamic attestation seems paradoxical, in the sense that the target binary could simply be part of the TEE itself. However, a major goal of TEEs is reducing the Trusted Computing Base (TCB); keeping the target binaries outside the immediate TCB significantly narrows the attack surface.

Acknowledgments. (i) This project has received funding from the European Research Council (ERC) under the European Union’s Horizon 2020 research and innovation programme (grant agreement No. 804476). (ii) This project has received funding by the ASCLEPIOS: Advanced Secure Cloud Encrypted Platform for Internationally Orchestrated Solutions in Healthcare Project No. 826093 EU research project. (iii) Supported in part by the Cybersecurity Research Award granted by the Technology Innovation Institute (TII). (iv) Supported in part by CSIC’s i-LINK+ 2019 “Advancing in cybersecurity technologies” (Ref. LINKA20216). (v) The first author was financially supported in part by HPY Research Foundation. (vi) M. C. Martínez-Rodríguez holds a postdoc that is co-funded by European Social Fund (ESF) and the Andalusian government, through the Andalucía ESF Operational Programme 2014–2020.

References

1. Abera, T., Asokan, N., Davi, L., Ekberg, J., Nyman, T., Paverd, A., Sadeghi, A., Tsudik, G.: C-FLAT: Control-flow attestation for embedded systems software. In: Weippl, E.R., Katzenbeisser, S., Kruegel, C., Myers, A.C., Halevi, S. (eds.) Proceedings of the 2016 ACM SIGSAC Conference on Computer and Communications Security, Vienna, Austria, October 24–28, 2016. pp. 743–754. ACM (2016), <https://doi.org/10.1145/2976749.2978358>
2. Castelluccia, C., Francillon, A., Perito, D., Soriente, C.: On the difficulty of software-based attestation of embedded devices. In: Al-Shaer, E., Jha, S., Keromytis, A.D. (eds.) Proceedings of the 2009 ACM Conference on Computer and Communications Security, CCS 2009, Chicago, Illinois, USA, November 9–13, 2009. pp. 400–409. ACM (2009), <https://doi.org/10.1145/1653662.1653711>
3. Chen, B., Dong, X., Bai, G., Jauhar, S., Cheng, Y.: Secure and efficient software-based attestation for industrial control devices with ARM processors. In: Proceedings of the 33rd Annual Computer Security Applications Conference, Orlando, FL, USA, December 4–8, 2017. pp. 425–436. ACM (2017), <https://doi.org/10.1145/3134600.3134621>
4. de Clercq, R., Keulenaer, R.D., Coppens, B., Yang, B., Maene, P., Bosschere, K.D., Preneel, B., Sutter, B.D., Verbauwhede, I.: SOFIA: Software and control flow integrity architecture. In: Fanucci, L., Teich, J. (eds.) 2016 Design, Automation &

Table 2. Complete statistics for every BEEBS benchmark used.

Benchmark	<i>COR_T</i> _{thres}	Max. FP	Precision	Recall	F1
aha-compress	0.7248	crc32 (23)	0.9617	0.7540	0.8453
bs	0.7096	newlib-sqrt (37)	0.9135	0.7710	0.8362
bubblesort	0.5312	nbody (30)	0.8959	0.7490	0.8159
cnt	0.7112	frac (3)	0.9775	0.6950	0.8124
cover	0.7264	crc (35)	0.9122	0.5820	0.7106
crc32	0.7447	aha-compress (9)	0.9783	0.5410	0.6967
crc	0.7724	duff (4)	0.9947	0.7570	0.8597
ctl-stack	0.6795	sqrt (50)	0.6018	0.8070	0.6895
ctl-vector	0.7070	ns (10)	0.9868	0.8200	0.8957
cubic	0.7232	sqrt (1)	0.9987	0.7890	0.8816
dijkstra	0.5141	nettle-des (1)	0.9986	0.7020	0.8244
duff	0.7318	crc (44)	0.9481	0.8040	0.8701
fasta	0.4935	bs (12)	0.9374	0.7340	0.8233
fibcall	0.6551	newlib-log (73)	0.6986	0.7370	0.7173
fir	0.6268	none	1.0000	0.8010	0.8895
frac	0.7856	crc32, newlib-sqrt (2)	0.9880	0.7420	0.8475
huffbench	0.5608	newlib-log (14)	0.8525	0.6360	0.7285
janne_complex	0.4192	crc (19)	0.8014	0.6860	0.7392
jfdctint	0.7598	nettle-des (48)	0.9360	0.7020	0.8023
lcdnum	0.3827	cnt (38)	0.6283	0.7100	0.6667
levenshtein	0.5909	template (4)	0.9904	0.7250	0.8372
matmult-float	0.7009	none	1.0000	0.6520	0.7893
matmult-int	0.4645	several operations (2)	0.9804	0.7520	0.8511
mergesort	0.7296	sglib-hashtable (44)	0.9058	0.6730	0.7722
nbody	0.5610	bubblesort (30)	0.8066	0.7130	0.7569
ndes	0.6663	nettle-aes (80)	0.8638	0.6340	0.7313
nettle-aes	0.6318	ndes (82)	0.8903	0.6900	0.7775
nettle-des	0.7444	cover (21)	0.9613	0.7690	0.8545
newlib-log	0.5017	dijkstra (78)	0.6399	0.6290	0.6344
newlib-sqrt	0.5191	dijkstra (81)	0.4573	0.7170	0.5584
ns	0.7599	none	1.0000	0.7320	0.8453
nsichneu	0.7869	none	1.0000	0.7210	0.8379
picojpeg	0.6009	st (13)	0.9805	0.6540	0.7846
qrduino	0.5639	sglib-listsort (6)	0.9834	0.4740	0.6397
rijndael	0.6470	ndes (5)	0.9927	0.6800	0.8071
select	0.6120	template (27)	0.9415	0.7880	0.8579
sglib-arrayheapsort	0.6372	bs (2)	0.9912	0.6720	0.8010
sglib-arrayquicksort	0.7020	mergesort (11)	0.9807	0.7110	0.8244
sglib-hashtable	0.6919	mergesort (77)	0.8894	0.6350	0.7410
sglib-listinsertsort	0.6251	various (1)	0.9947	0.7540	0.8578
sglib-listsort	0.5108	qrduino (24)	0.9492	0.6540	0.7744
sqrt	0.5113	rijndael (2)	0.9923	0.6470	0.7833
st	0.5812	picojpeg (24)	0.9644	0.6770	0.7955
stb_perlin	0.6476	template (3)	0.9833	0.6460	0.7797
tarai	0.6927	wikisort (37)	0.9025	0.7500	0.8192
template	0.6654	select (19)	0.9487	0.6840	0.7949
wikisort	0.7092	sglib-listinsertsort (9)	0.9673	0.7090	0.8182

- Test in Europe Conference & Exhibition, DATE 2016, Dresden, Germany, March 14-18, 2016. pp. 1172–1177. IEEE (2016), <http://ieeexplore.ieee.org/document/7459489/>
5. Coker, G., Guttman, J.D., Loscocco, P., Herzog, A.L., Millen, J.K., O’Hanlon, B., Ramsdell, J.D., Segall, A., Sheehy, J., Sniffen, B.T.: Principles of remote attestation. *Int. J. Inf. Sec.* 10(2), 63–81 (2011), <https://doi.org/10.1007/s10207-011-0124-7>
 6. Dessouky, G., Zeitouni, S., Nyman, T., Paverd, A., Davi, L., Koeberl, P., Asokan, N., Sadeghi, A.: LO-FAT: Low-overhead control flow attestation in hardware. In: Proceedings of the 54th Annual Design Automation Conference, DAC 2017, Austin, TX, USA, June 18-22, 2017. pp. 24:1–24:6. ACM (2017), <https://doi.org/10.1145/3061639.3062276>
 7. Dolev, D., Yao, A.C.: On the security of public key protocols. *IEEE Trans. Inf. Theory* 29(2), 198–207 (1983), <https://doi.org/10.1109/TIT.1983.1056650>
 8. Gnad, D.R.E., Krautter, J., Tahoori, M.B.: Leaky noise: New side-channel attack vectors in mixed-signal IoT devices. *IACR Trans. Cryptogr. Hardw. Embed. Syst.* 2019(3), 305–339 (2019), <https://doi.org/10.13154/tches.v2019.i3.305-339>
 9. Gnad, D.R.E., Krautter, J., Tahoori, M.B., Schellenberg, F., Moradi, A.: Remote electrical-level security threats to multi-tenant FPGAs. *IEEE Des. Test* 37(2), 111–119 (2020), <https://doi.org/10.1109/MDAT.2020.2968248>
 10. Goldwasser, S., Micali, S., Rivest, R.L.: A digital signature scheme secure against adaptive chosen-message attacks. *SIAM J. Comput.* 17(2), 281–308 (1988), <https://doi.org/10.1137/0217017>
 11. Gravellier, J., Dutertre, J., Teglia, Y., Loubet-Moundi, P.: High-speed ring oscillator based sensors for remote side-channel attacks on FPGAs. In: Andrews, D., Cumplido, R., Feregrino, C., Platzner, M. (eds.) 2019 International Conference on ReConFigurable Computing and FPGAs, ReConFig 2019, Cancun, Mexico, December 9-11, 2019. pp. 1–8. IEEE (2019), <https://doi.org/10.1109/ReConFig48160.2019.8994789>
 12. Gravellier, J., Dutertre, J., Teglia, Y., Loubet-Moundi, P., Olivier, F.: Remote side-channel attacks on heterogeneous SoC. In: Belaïd, S., Güneysu, T. (eds.) Smart Card Research and Advanced Applications - 18th International Conference, CARDIS 2019, Prague, Czech Republic, November 11-13, 2019, Revised Selected Papers. *Lecture Notes in Computer Science*, vol. 11833, pp. 109–125. Springer (2019), https://doi.org/10.1007/978-3-030-42068-0_7
 13. Han, Y., Etigowni, S., Liu, H., Zonouz, S.A., Petropulu, A.P.: Watch me, but don’t touch me! contactless control flow monitoring via electromagnetic emanations. In: Thuraisingham, B.M., Evans, D., Malkin, T., Xu, D. (eds.) Proceedings of the 2017 ACM SIGSAC Conference on Computer and Communications Security, CCS 2017, Dallas, TX, USA, October 30 - November 03, 2017. pp. 1095–1108. ACM (2017), <https://doi.org/10.1145/3133956.3134081>
 14. Lee, D., Kohlbrenner, D., Shinde, S., Asanovic, K., Song, D.: Keystone: an open framework for architecting trusted execution environments. In: Bilas, A., Magoutis, K., Markatos, E.P., Kostic, D., Seltzer, M. (eds.) EuroSys ’20: Fifteenth EuroSys Conference 2020, Heraklion, Greece, April 27-30, 2020. pp. 38:1–38:16. ACM (2020), <https://doi.org/10.1145/3342195.3387532>
 15. Li, Y., McCune, J.M., Perrig, A.: VIPER: verifying the integrity of peripherals’ firmware. In: Chen, Y., Danezis, G., Shmatikov, V. (eds.) Proceedings of the 18th ACM Conference on Computer and Communications Security, CCS 2011, Chicago, Illinois, USA, October 17-21, 2011. pp. 3–16. ACM (2011), <https://doi.org/10.1145/2046707.2046711>

16. Lipp, M., Kogler, A., Oswald, D., Schwarz, M., Easdon, C., Canella, C., Gruss, D.: PLATYPUS: Software-based power side-channel attacks on x86. In: 2021 IEEE Symposium on Security and Privacy, SP 2021, Proceedings, 23-27 May 2021, Virtual Event. pp. 1080–1096. IEEE Computer Society (2021), <https://doi.ieeecomputersociety.org/10.1109/SP40001.2021.00063>
17. Lisovets, O., Knichel, D., Moos, T., Moradi, A.: Let’s take it offline: Boosting brute-force attacks on iPhone’s user authentication through SCA. *IACR Trans. Cryptogr. Hardw. Embed. Syst.* 2021(3), 496–519 (2021), <https://doi.org/10.46586/tches.v2021.i3.496-519>
18. Liu, H., Vasserman, E.Y.: Gray-box software integrity checking via side-channels. In: Lin, X., Ghorbani, A., Ren, K., Zhu, S., Zhang, A. (eds.) *Security and Privacy in Communication Networks - 13th International Conference, SecureComm 2017, Niagara Falls, ON, Canada, October 22-25, 2017, Proceedings. Lecture Notes of the Institute for Computer Sciences, Social Informatics and Telecommunications Engineering*, vol. 238, pp. 3–23. Springer (2017), https://doi.org/10.1007/978-3-319-78813-5_1
19. Martínez-Rodríguez, M.C., Delgado-Lozano, I.M., Brumley, B.B.: SoK: Remote power analysis. In: Reinhardt, D., Müller, T. (eds.) *ARES 2021: The 16th International Conference on Availability, Reliability and Security, Vienna, Austria, August 17-20, 2021*. pp. 7:1–7:12. ACM (2021), <https://doi.org/10.1145/3465481.3465773>
20. Msgna, M., Markantonakis, K., Naccache, D., Mayes, K.: Verifying software integrity in embedded systems: A side channel approach. In: Prouff, E. (ed.) *Constructive Side-Channel Analysis and Secure Design - 5th International Workshop, COSADE 2014, Paris, France, April 13-15, 2014. Revised Selected Papers. Lecture Notes in Computer Science*, vol. 8622, pp. 261–280. Springer (2014), https://doi.org/10.1007/978-3-319-10175-0_18
21. Nazari, A., Sehatbakhsh, N., Alam, M., Zajic, A.G., Prvulovic, M.: EDDIE: EM-based detection of deviations in program execution. In: *Proceedings of the 44th Annual International Symposium on Computer Architecture, ISCA 2017, Toronto, ON, Canada, June 24-28, 2017*. pp. 333–346. ACM (2017), <https://doi.org/10.1145/3079856.3080223>
22. O’Flynn, C., Dewar, A.: On-device power analysis across hardware security domains. *IACR Trans. Cryptogr. Hardw. Embed. Syst.* 2019(4), 126–153 (2019), <https://doi.org/10.13154/tches.v2019.i4.126-153>
23. Pallister, J., Hollis, S.J., Bennett, J.: BEEBS: Open benchmarks for energy measurements on embedded platforms. *CoRR abs/1308.5174* (2013), <http://arxiv.org/abs/1308.5174>
24. Pallister, J., Hollis, S.J., Bennett, J.: Identifying compiler options to minimize energy consumption for embedded platforms. *Comput. J.* 58(1), 95–109 (2015), <https://doi.org/10.1093/comjnl/bxt129>
25. Ramesh, C., Patil, S.B., Dhanuskodi, S.N., Provelengios, G., Pillement, S., Holcomb, D.E., Tessier, R.: FPGA side channel attacks without physical access. In: *26th IEEE Annual International Symposium on Field-Programmable Custom Computing Machines, FCCM 2018, Boulder, CO, USA, April 29 - May 1, 2018*. pp. 45–52. IEEE Computer Society (2018), <https://doi.org/10.1109/FCCM.2018.00016>
26. Schellenberg, F., Gnad, D.R.E., Moradi, A., Tahoori, M.B.: An inside job: Remote power analysis attacks on FPGAs. In: Madsen, J., Coskun, A.K. (eds.) *2018 Design, Automation & Test in Europe Conference & Exhibition, DATE 2018, Dresden,*

- Germany, March 19-23, 2018. pp. 1111–1116. IEEE (2018), <https://doi.org/10.23919/DATE.2018.8342177>
27. Schellenberg, F., Gnad, D.R.E., Moradi, A., Tahoori, M.B.: Remote inter-chip power analysis side-channel attacks at board-level. In: Bahar, I. (ed.) Proceedings of the International Conference on Computer-Aided Design, ICCAD 2018, San Diego, CA, USA, November 05-08, 2018. p. 114. ACM (2018), <https://doi.org/10.1145/3240765.3240841>
 28. Sehatbakhsh, N., Nazari, A., Khan, H.A., Zajic, A.G., Prvulovic, M.: EMMA: Hardware/software attestation framework for embedded systems using electromagnetic signals. In: Proceedings of the 52nd Annual IEEE/ACM International Symposium on Microarchitecture, MICRO 2019, Columbus, OH, USA, October 12-16, 2019. pp. 983–995. ACM (2019), <https://doi.org/10.1145/3352460.3358261>
 29. Seshadri, A., Luk, M., Perrig, A., van Doorn, L., Khosla, P.K.: Pioneer: Verifying code integrity and enforcing untampered code execution on legacy systems. In: Christodorescu, M., Jha, S., Maughan, D., Song, D., Wang, C. (eds.) Malware Detection, Advances in Information Security, vol. 27, pp. 253–289. Springer (2007), https://doi.org/10.1007/978-0-387-44599-1_12
 30. Seshadri, A., Luk, M., Perrig, A., van Doorn, L., Khosla, P.K.: SCUBA: Secure code update by attestation in sensor networks. In: Poovendran, R., Juels, A. (eds.) Proceedings of the 2006 ACM Workshop on Wireless Security, Los Angeles, California, USA, September 29, 2006. pp. 85–94. ACM (2006), <https://doi.org/10.1145/1161289.1161306>
 31. Seshadri, A., Perrig, A., van Doorn, L., Khosla, P.K.: SWATT: Software-based attestation for embedded devices. In: 2004 IEEE Symposium on Security and Privacy (S&P 2004), 9-12 May 2004, Berkeley, CA, USA. p. 272. IEEE Computer Society (2004), <https://doi.org/10.1109/SECPRI.2004.1301329>
 32. Yang, S., Alaql, A., Hoque, T., Bhunia, S.: Runtime integrity verification in cyber-physical systems using side-channel fingerprint. In: IEEE International Conference on Consumer Electronics, ICCE 2019, Las Vegas, NV, USA, January 11-13, 2019. pp. 1–6. IEEE (2019), <https://doi.org/10.1109/ICCE.2019.8662071>
 33. Zhao, M., Suh, G.E.: FPGA-based remote power side-channel attacks. In: 2018 IEEE Symposium on Security and Privacy, SP 2018, Proceedings, 21-23 May 2018, San Francisco, California, USA. pp. 229–244. IEEE Computer Society (2018), <https://doi.org/10.1109/SP.2018.00049>